Nonlinear Dyn
DOI 10.1007/s11071-017-3915-1

ORIGINAL ARTICLE

Adaptive optimal control of multi-modular floating platforms in random seas

Daolin Xu · Shuyan Xia · Haicheng Zhang · Yousheng Wu

Received: 2 September 2017 / Accepted: 30 October 2017

Abstract This paper presents an adaptive optimal control method to suppress the oscillation of a floating platforms system in random seas. The system consists of multiple modules which are connected by flexible connectors with strong geometrical nonlinearity. To cope with the uncertain waves, a disturbance estimator is introduced to assess the actual wave excitation. This adaptive scheme of the estimator is integrated with an optimal control method subject to a limitation on the control outputs of actuators, where the optimal control process is carried out by the sequential quadratic program method. In numerical experiments, a floating platform with five semi-submersible modules is considered. Control process deals with 20 control variables to stabilize the surge, sway and yaw motions of a 30-DOF floating system, subject to unknown irregular waves and limitation of control output. Numerical results have verified the efficiency of the control strategy and show that the proposed control method performs very well.

Keywords Multi-modular floating platform · Uncertain wave disturbance · High-dimensional nonlinearity · Adaptive optimal control

D. Xu (✉) · S. Xia · H. Zhang
State Key Laboratory of Advanced Design and Manufacturing for Vehicle Body, College of Mechanical and Vehicle Engineering, Hunan University, Changsha 410082, People's Republic of China
e-mail: dlxu@hnu.edu.cn

S. Xia
e-mail: syxia@hnu.edu.cn

H. Zhang
e-mail: zhanghc@hnu.edu.cn

Y. Wu
China Ship Scientific Research Center, Wuxi 214082, People's Republic of China
e-mail: wuys@cssrc.com.cn

1 Introduction

The pressure of the rapid growth of population, progress of industry and exclusive cost of lands triggered the motivation of developing very large floating structures (VLFS) deployed in relatively unused sea and ocean spaces. Comparing with the traditional land reclamation solution, VLFS have more advantages such as environmental friendly, easy construction and fast deployment and expansion [1]. The applications of VLFS could include floating piers, floating hotels, floating fuel storage facilities, floating nuclear power station, floating bridges, floating airports and even floating cities [2]. In 1990s, two notable projects of the Mega-Float and the Mobile Offshore Base (MOB) were launched by Japanese and American governments [3]. They have activated a great mount of the enthusiasm from researchers and engineers in the field of ocean engineering. A large number of research works have been documented with the aid of the hydroelastic theory [4,5] which is particularly dealing with fluid–structure interaction [6]. These works laid the foundation of the methodology in the dynamic forecasting of VLFS in

Published online: 12 November 2017

sea conditions. Some typical examples are given as follows: a single plate model for pontoon-type VLFS in linear wave conditions [7], multi-modular VLFS in regular waves [8], semi-submersible module in random sea [9], etc.

Dynamic control of floating structures is very much concerned in marine engineering. There are abundant references for motion control of various marine systems, to enhance the efficiency of wave energy conversion [10,11], to stabilize the motions of vessels [12,13] and floating platforms [14,15], floating wind turbine [16], offshore steel jacked platforms [15,17] and tension leg platform [18]. Dynamic positioning (DP) [19] is an important part of control techniques mainly used to manipulate the position or predetermine track of floating platforms through active thrusters. A large number of articles about DP have been documented about the control methods and related experiments [20–23]. For MOB modules, Manikonda [24] and Rahman [25] used model predictive control to coordinate the dynamic position. The former article dealt with the uncertain disturbance of environment by a linearization technique. However, the work on the active control for the oscillation suppression of large floating structures is relatively rare. For the Mega-Float, a pneumatic-type active control apparatus was studied to dampen wave-induced heave motions and the deflections of the floating structure [26]. Very recently, a new approach [27] is developed to stabilize the motions of VLFS by adjusting the connector stiffness based on the network concept of "amplitude death," which permits a weak oscillatory state [28].

To control the oscillation of multi-modular VLFS, one may confront the toughness of dealing with high-dimensional nonlinearity. In addition, stabilization of complicated VLFS systems requires collaborative manipulations among a number of actuators installed, and further complex environmental conditions in seas make the study challenging. In this paper, we aims to suppress the most threatening motions of multi-modular floating structures by using an adaptive optimal control, subject to disturbances of uncertain waves and limitations of control outputs. The work may enrich the study in the field of oscillation control of multi-modular VLFS, which has been rarely investigated.

This paper is organized as follows. In the next section, the configuration of the multi-modular floating structure is elaborated and the mathematical model is developed by using the network theory. In the third section, firstly a disturbance observer is introduced to estimate irregular wave load and followed with an optimal control to determine the output of actuators. In numerical experiments, parameters of a five-modular floating platform and wave conditions are provided, and the adaptive control method is numerically verified. Finally a conclusion is drawn.

2 Mathematical model of floating systems with control

A floating platform is comprised by N number of floating modules as shown in Fig. 1, where the modules are sequentially connected by spring connectors. The modules are also constrained by anchor chains to prevent the floating structure from drifting. A global coordinate system (x, y, z) is set on the still water surface of the earth where x axis points to the longitudinal direction and y axis lies in the transversal direction of the floating structure; z axis is perpendicular to still water surface. Further a local coordinate system (X, Y, Z, AX, AY, AZ) is fixed at the mass center of each module as shown in Fig. 1. All modules are assumed to be symmetrical to x and y axes. The rotation center of a module is coincident with the center of mass. The wave angle is defined by the angle between x axis and the direction of wave propagation. To suppress the oscillation of modules, each module is equipped with two propellers which can be independently turned to any direction to provide thrusts in X–Y plane.

Based on the network modeling method [29], the motion equation of the whole floating system can be integrated by the model of single floating module, model of connectors, model of wave force and model of mooring system. The dynamic model of the floating structure with control is briefly written by a set of first-order ordinary differential equations as follows

$$\begin{aligned}
\dot{\mathbf{x}}_{1,i} &= \mathbf{x}_{2,i} \\
\dot{\mathbf{x}}_{2,i} &= \frac{1}{\mathbf{M}_i}\Bigg(-(\mathbf{S}_i + \mathbf{D}_i)\mathbf{x}_{1,i} + \mathbf{f}_{w,i}(\omega, a, \theta, \mathbf{x}_2, \dot{\mathbf{x}}_2) \\
&\qquad + \varepsilon \sum_{j=1}^{N} \left(\mathbf{\Phi}_{ij} K(\mathbf{x}_{1,i}, \mathbf{x}_{1,j})\right) + H(\mathbf{u}_i) \Bigg) \\
&\qquad i = 1, \ldots, N
\end{aligned} \tag{1}$$

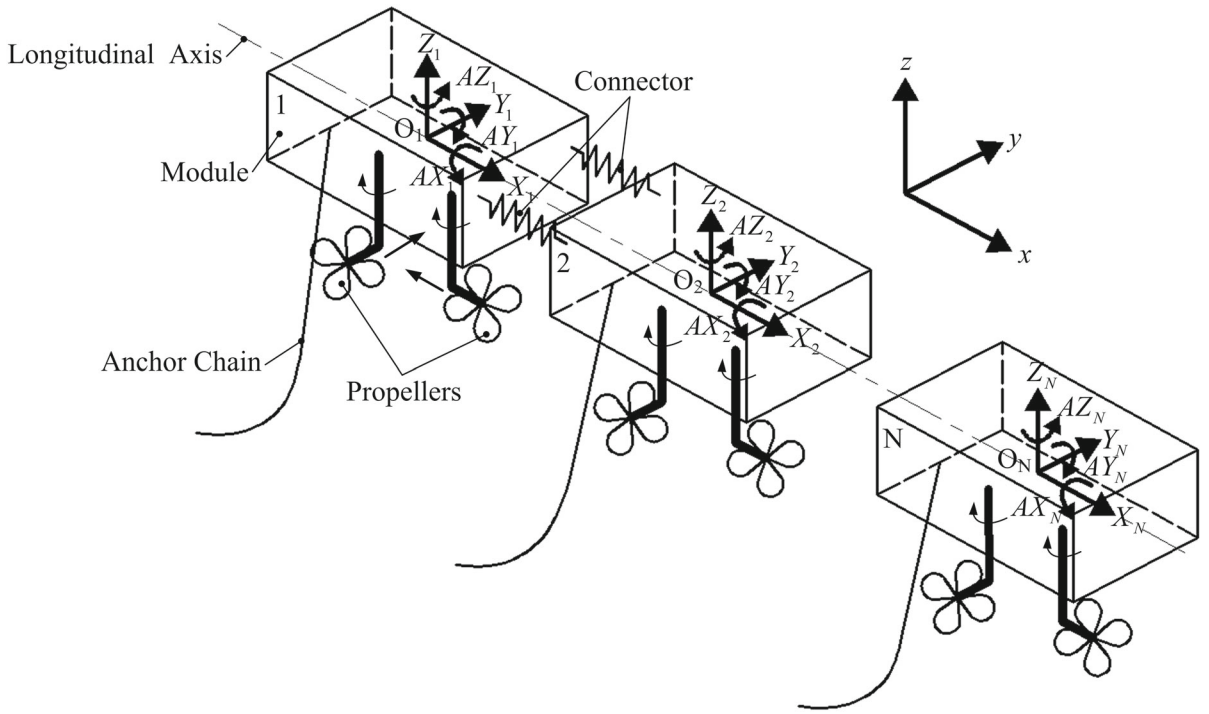

Fig. 1 Schematic diagram of the chain-type multi-modular floating platforms

where $\mathbf{x}_{1,i} = [x_i, y_i, z_i, \alpha_i, \beta_i, \gamma_i]^{\mathrm{T}}$ is the displacement vector of the ith module, which represents the motions of surge, sway, heave, roll, pitch and yaw, respectively. Symbol $\mathbf{x}_{2,i} = [\dot{x}_i, \dot{y}_i, \dot{z}_i, \dot{\alpha}_i, \dot{\beta}_i, \dot{\gamma}_i]^{\mathrm{T}}$ is the velocity of $\mathbf{x}_{1,i}$. Symbols $\mathbf{M}_i \in \mathbb{R}^{6\times6}$, $\mathbf{S}_i \in \mathbb{R}^{6\times6}$ and $\mathbf{D}_i \in \mathbb{R}^{6\times6}$ are the mass matrix, linear restoring force matrix of water and mooring stiffness matrix. Wave force $\mathbf{f}_{w,i}(\omega, a, \theta, \mathbf{x}_2, \dot{\mathbf{x}}_2) \in \mathbb{C}^{6\times1}$ is a function of wave frequency ω, wave height a and wave angle θ. The effect of wave diffraction is also considered, which is related to the velocity and acceleration of the state of the floating platform. The term $\varepsilon \sum_{j=1}^{N} \left(\Phi_{ij} K\left(\mathbf{x}_{1,i}, \mathbf{x}_{1,j}\right)\right)$ denotes the connector forces imposed on the ith module. Symbol ε is the stiffness of the connectors and $\Phi \in \mathbb{R}^{6\times6}$ is the topological matrix defining the coupling relationship of the ith module and the jth module. The function $K\left(\mathbf{x}_{1,i}, \mathbf{x}_{1,j}\right) \in \mathbb{R}^{6\times1}$ expresses the relative displacement vector between the mass centers of the ith module and the jth module. The derivation processes of the terms mentioned above are given in "Appendix".

The last term $H(\mathbf{u}_i)$ particularly relates to the controlled thrusts of propellers mounted to the ith module. There are four control variables $\mathbf{u}_i = [u_{1,i}, u_{2,i}, \theta_{1,i}, \theta_{2,i}]$ for each module in which symbols $u_{1,i}$ and $u_{2,i}$ represent the output control forces of two propellers, respectively, and symbols $\theta_{1,i}$ and $\theta_{2,i}$ are the turning angles referring to y axis of the global coordinate system. Without the wave excitation, the initial position of the mass center of the ith module is located at the point of $\mathbf{p}_{0,i}$ in the global coordinate system, while the two propellers are installed at the points $\mathbf{p}_{u10,i}$ and $\mathbf{p}_{u20,i}$ in the local coordinate system. With the wave excitation, the mass center of the floating module moves to $\mathbf{p}_{a,i} = \mathbf{p}_{0,i} + [x_i, y_i, z_i]^{\mathrm{T}}$ in the global coordinate, and the two propellers are shifted to the positions of

$$\begin{aligned} \mathbf{p}_{u1a,i} &= \mathbf{p}_{a,i} + \mathrm{tran}(\alpha_i, \beta_i, \gamma_i) \cdot \mathbf{p}_{u10,i} \\ \mathbf{p}_{u2a,i} &= \mathbf{p}_{a,i} + \mathrm{tran}(\alpha_i, \beta_i, \gamma_i) \cdot \mathbf{p}_{u20,i} \end{aligned} \tag{2}$$

where $\mathrm{tran}(\cdot)$ is a coordinate transfer function [30] expressed as

$$\text{tran}(\alpha,\beta,\gamma)=\begin{bmatrix}\text{co}\gamma\text{s}\cos\beta & -\sin\gamma\cos\alpha+\cos\gamma\sin\beta\sin\alpha & \sin\gamma\sin\alpha+\cos\gamma\cos\alpha\sin\beta\\ \sin\gamma\cos\beta & \cos\beta\cos\alpha+\sin\alpha\sin\beta\sin\gamma & -\cos\gamma\sin\alpha+\sin\beta\sin\gamma\cos\alpha\\ -\sin\beta & \cos\beta\sin\alpha & \cos\beta\cos\alpha\end{bmatrix} \tag{3}$$

The vectors from the points where the propeller thrusts are applied to the mass center are

$$\begin{aligned}\mathbf{b}_{u1,i}&=\mathbf{p}_{u1a,i}-\mathbf{p}_{a,i}\\ \mathbf{b}_{u2,i}&=\mathbf{p}_{u2a,i}-\mathbf{p}_{a,i}\end{aligned} \tag{4}$$

The control forces of two propellers imposed on the mass center can be expressed by

$$\begin{aligned}\mathbf{f}_{u1,i}&=[u_{1,i}\sin\left(\theta_{1,i}\right),u_{1,i}\cos\left(\theta_{1,i}\right),0]^{\mathrm{T}}\\ \mathbf{f}_{u2,i}&=[u_{2,i}\sin\left(\theta_{2,i}\right),u_{2,i}\cos\left(\theta_{2,i}\right),0]^{\mathrm{T}}\end{aligned} \tag{5}$$

Then the force moments acting on the mass center are

$$\begin{aligned}\mathbf{m}_{u1,i}&=\mathbf{b}_{u1,i}\times\mathbf{f}_{u1,i}\\ \mathbf{m}_{u2,i}&=\mathbf{b}_{u2,i}\times\mathbf{f}_{u2,i}\end{aligned} \tag{6}$$

The expression of the control force vector $H(\mathbf{u}_i)$ can be written as

$$H(\mathbf{u}_i)=\left[\mathbf{f}_{u1,i}+\mathbf{f}_{u2,i},\mathbf{m}_{u1,i}+\mathbf{m}_{u2,i}\right]^{\mathrm{T}} \tag{7}$$

Remark that small displacements of the modules may cause large displacements at the points of connections because the size of modules is much larger than the size of connectors. The large displacements of the connectors could induce significant geometrical nonlinearity into the dynamic model of the floating structure. In addition, the control term defined by Eq. (5) contains large turning angles making the control force defined in Eq. (7) to be nonlinear. Without the control term in the dynamic model (1), due to the geometric nonlinearity of connectors, the floating platform may evolve into large oscillatory states under wave excitations, such as sudden leaps [31] from a wave frequency-dependent harmonic motion to chaotic or multiple sub-harmonic motions [32].

The purpose of this paper is to employ this controller in Eq. (7) to suppress the oscillation of the floating structure in uncertain waves. It requires to manage a number of propellers in a cooperative way to cope with a high-dimensional nonlinear control problem. For more realistic applications, unknown irregular waves and the saturation of control output will be concerned in the development of the control strategy.

3 Adaptive optimal control strategy

The statistic characteristic of waves in a sea state is usually described by wave spectrum. JONSWAP spectrum [33] is popular one often used in marine engineering, given by

$$S_\eta(\omega)=\zeta H_s^2\omega_p^4\omega^{-5}\exp\left(-1.25\omega_p^4\omega^{-4}\right)\kappa^{\exp\left(-\frac{(\omega-\omega_p)^2}{2\sigma^2\omega_p^2}\right)} \tag{8}$$

where $\zeta, H_s, \omega_p, \kappa$ and σ are the dimensional constant, the significant wave height, the dominant wave frequency, the peak enhancement factor and the peak shape parameter, respectively. We consider the multi-module floating system to be deployed in irregular waves. The irregular waves can be approximately expressed by a dominant regular wave with many individual wave components so that the combined wave height is random, which can be derived from the JONSWAP spectrum [34]. The derivation of the wave excitation is displayed in "Appendix." In numerical simulations, the floating system will be excited by irregular waves, where the wave excitation is treated as an unknown disturbance to the system during a control process. In what follows, we are going to develop an adaptive scheme to estimate the wave disturbance along with the control process.

Consider the wave disturbance in the equation of motion Eq. (1) and rewrite the equation as

$$\begin{aligned}\dot{\mathbf{x}}_{1,i}&=\mathbf{x}_{2,i}\\ \dot{\mathbf{x}}_{2,i}&=\boldsymbol{\varphi}_i+\mathbf{d}_i\ \ i=1,\ldots N\end{aligned} \tag{9}$$

where symbol $\mathbf{d}_i=[d_{1,i},\ldots,d_{6,i}]^{\mathrm{T}}$ denotes the actual wave disturbance imposed on the ith modal, given by

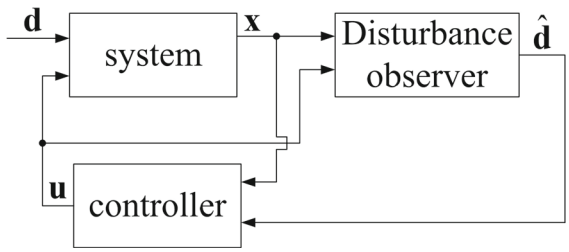

Fig. 2 Flowchart of control process

$$\mathbf{d}_i = \frac{1}{\mathbf{M}_i}\mathbf{f}_{w,i}\left(\omega, a, \theta, \mathbf{x}_2, \dot{\mathbf{x}}_2\right)$$

$$\boldsymbol{\varphi}_i = \frac{1}{\mathbf{M}_i}\left(-\left(\mathbf{S}_i + \mathbf{D}_i\right)\mathbf{x}_{1,i} + \varepsilon \sum_{j=1}^{N}\left(\boldsymbol{\Phi}_{ij} K\left(\mathbf{x}_{1,i}, \mathbf{x}_{1,j}\right)\right) + H\left(\mathbf{u}_i\right)\right) \quad i = 1, \ldots N \tag{10}$$

A disturbance observer will be introduced to estimate the actual wave disturbance. Thus the control process can be briefly expressed by the flowchart in Fig. 2.

The disturbance observer generates an estimated value $\hat{\mathbf{d}}$ of the actual disturbance $\mathbf{d}_i$. The estimated disturbance together with the state $\mathbf{x}$ will be fed into the controller to generate propeller output $\mathbf{u}$ that is applied to the floating system. The control is conducted in an iterative way, where the current control step is based on the results of the previous step so that to carry out an adaptive control process. During this control process, the wave disturbance will be improvingly estimated.

To design a suitable disturbance observer, firstly assume the wave disturbance as an unknown constant force vector. This assumption will certainly bring error to the estimator of the real disturbance. But this error can be reduced and even eliminated if design parameters of the disturbance observer are properly set.

Referring to the article [35], we introduce linear filters $G_i(s) = [G_{1,i}(s), \ldots, G_{6,i}(s)]^{\mathrm{T}}$ to all degrees of freedom for the ith floating module, defined by

$$G_{j,i}(s) = \frac{1}{1 + s\tau_{j,i}} \quad j = 1, \ldots 6, \quad i = 1, \ldots N \tag{11}$$

where $\tau_{1,i}, \ldots, \tau_{6,i}$ are positive parameters to be determined and s is the variable of Laplace transformation. With the filters, the disturbance observer is designed in a form of differential equation, given by

$$\operatorname{diag}(\boldsymbol{\tau}_i) \cdot \dot{\hat{\mathbf{d}}}_i + \hat{\mathbf{d}}_i = \mathbf{d}_i \quad i = 1, \ldots N \tag{12}$$

where $\operatorname{diag}(\cdot)$ is a diagonal matrix with diagonal elements $\boldsymbol{\tau}_i = \left[\tau_{1,i}, \ldots, \tau_{6,i}\right]$. Since $\mathbf{d}_i$ is regarded as a constant, the solution of the estimated disturbance can be derived as

$$\hat{\mathbf{d}}_i = \mathbf{d}_i - \exp\left(-\left(\boldsymbol{\tau}_i\right)^{-1} t\right) \tag{13}$$

As long as the elements of vector $\boldsymbol{\tau}_i$ are positive, the exponential term will be vanished in time evolution. The solution of Eq. (13) tends to $\hat{\mathbf{d}}_i \Rightarrow \mathbf{d}_i$. Note that the rate of convergence from the estimated disturbance $\hat{\mathbf{d}}_i$ to the real disturbance $\mathbf{d}_i$ is dependent on the setting of the positive parameters $\tau_{1,i}, \ldots, \tau_{6,i}$.

Based on the disturbance observer shown in Eq. (12), we next determine the parametric vector $\boldsymbol{\tau}_i$ [36] so as to make the adaptive law Eq. (13) feasible in control feedback loop. Therefore, we introduce a state-dependent form for the solution of Eq. (12), given by

$$\hat{\mathbf{d}}_i = \mathbf{d}_i - \exp\left(-\left(\boldsymbol{\tau}_i\right)^{-1} t\right) = \mathbf{w}_i + \mathbf{p}_i\left(\mathbf{x}_{2,i}\right) \quad i = 1, \ldots N \tag{14}$$

where $\mathbf{w}_i = [w_{1,i}, \ldots, w_{6,i}]^{\mathrm{T}}$ and $\mathbf{p}_i = [p_{1,i}, \ldots, p_{6,i}]^{\mathrm{T}}$ are state-dependent functions to be designed. Differentiating Eq. (14) with respect to time and substituting Eq. (9), it results in

$$\dot{\hat{\mathbf{d}}}_i = \operatorname{diag}\left(\left(\boldsymbol{\tau}_i\right)^{-1}\right) \cdot \exp\left(-\left(\boldsymbol{\tau}_i\right)^{-1} t\right) = \dot{\mathbf{w}}_i + \frac{\partial \mathbf{p}_i}{\partial \mathbf{x}_{2,i}}\left(\boldsymbol{\varphi}_i + \mathbf{d}_i\right) \quad i = 1, \ldots N \tag{15}$$

From Eq. (14), we have $\exp\left(-\left(\boldsymbol{\tau}_i\right)^{-1} t\right) = \mathbf{d}_i - \mathbf{w}_i - \mathbf{p}_i\left(\mathbf{x}_{2,i}\right)$ which is submitted into Eq. (15) and gets

$$\operatorname{diag}\left(\left(\boldsymbol{\tau}_i\right)^{-1}\right) \cdot \left(\mathbf{d}_i - \mathbf{w}_i - \mathbf{p}_i\left(\mathbf{x}_{2,i}\right)\right) = \dot{\mathbf{w}}_i + \frac{\partial \mathbf{p}_i}{\partial \mathbf{x}_{2,i}}\left(\boldsymbol{\varphi}_i + \mathbf{d}_i\right) \quad i = 1, \ldots N \tag{16}$$

To make Eq. (16) hold true, we require the following equality

$$\operatorname{diag}\left(\left(\boldsymbol{\tau}_i\right)^{-1}\right) = \frac{\partial \mathbf{p}_i}{\partial \mathbf{x}_{2,i}}$$

$$\dot{\mathbf{w}}_i = -\frac{\partial \mathbf{p}_i}{\partial \mathbf{x}_{2,i}}\left(\boldsymbol{\varphi}_i\left(\mathbf{x}_1, \mathbf{u}_i\right) + \mathbf{w}_i + \mathbf{p}_i\left(\mathbf{x}_{2,i}\right)\right) \quad i = 1, \ldots N \tag{17}$$

As discussed above, the elements of $\boldsymbol{\tau}_i$ have to be set positive to guarantee the estimated disturbance $\hat{\mathbf{d}}_i$

asymptotically converging to the real disturbance $\mathbf{d}_i$. From the first equation of Eq. (17), we can design the function $\mathbf{p}_i$ as

$$\mathbf{p}_i = \kappa \mathbf{l}_i \left[\dot{x}_i + (\dot{x}_i)^3 , \dot{y}_i + (\dot{y}_i)^3 , \dot{z}_i + (\dot{z}_i)^3 , \dot{\alpha}_i + (\dot{\alpha}_i)^3 , \dot{\beta}_i + \left(\dot{\beta}_i\right)^3 , \dot{\gamma}_i + (\dot{\gamma}_i)^3 \right]^{\mathrm{T}} \quad i = 1, \ldots N \tag{18}$$

where κ is a positive number and $\mathbf{l}_i$ is unity matrix. The elements of $\frac{\partial \mathbf{p}_i}{\partial \mathbf{x}_{2,i}}$ are all positive greater than κ. We can achieve faster convergence rate if κ is set to larger. Note that there is great flexibility to design the function $\mathbf{p}_i$ as long as its partial differential with respect to state variables is positive. By so doing, the adaptive scheme in Eq. (12) is associated with the state variables so that this adaptive scheme can be integrated with a state feedback control program.

Remark that the above derivation is based on the prerequisite that the wave disturbance is constant, i.e., $\dot{\mathbf{d}}_i = 0$. This assumption may introduce errors in the estimation process of wave disturbance. If $\mathbf{d}_i$ is time dependent, the estimated error can be written as

$$\tilde{\mathbf{d}}_i = \mathbf{d}_i - \hat{\mathbf{d}}_i \; i = 1, \ldots N \tag{19}$$

Substituting Eq. (19) into Eq. (12), it yields

$$\mathrm{diag}\,(\boldsymbol{\tau}_i) \cdot \dot{\tilde{\mathbf{d}}}_i + \tilde{\mathbf{d}}_i = \mathrm{diag}\,(\boldsymbol{\tau}_i) \cdot \dot{\mathbf{d}}_i \quad i = 1, \ldots N \tag{20}$$

which leads to the solution

$$\tilde{\mathbf{d}}_i = \mathrm{diag}\,(\boldsymbol{\tau}_i) \cdot \dot{\mathbf{d}}_i - \exp\left(-(\boldsymbol{\tau}_i)^{-1} t\right) \tag{21}$$

It indicates that the estimated error $\tilde{\mathbf{d}}_i$ is related to the change in rate of real disturbance $\dot{\mathbf{d}}_i$. Suppose $\dot{\mathbf{d}}_i$ is confined within the inequality $\left|\dot{\mathbf{d}}_i\right| \leq \boldsymbol{\xi}$ which is a possible maximum change in rate of error. As time goes by, the second term in the right-hand side of Eq. (21) will be vanished. The estimated error is within the range of $\left|\tilde{\mathbf{d}}_i\right| \leq \mathrm{diag}\,(\boldsymbol{\tau}_i) \cdot \boldsymbol{\xi}$. It implies that smaller $\boldsymbol{\tau}_i$ can lead to less error of the estimation. Thus we can choose the parameters of $\boldsymbol{\tau}_i$ as smaller as possible by designing a larger number of κ. Alternatively one can also use a higher-order filter. Interested readers can also refer to the article [35] where the estimated error for the second-order filters is bounded by $\left|\tilde{\mathbf{d}}_i\right| \leq (\boldsymbol{\tau}_i)^2 \boldsymbol{\xi}$.

The purpose of the control in this paper is to minimize the unwanted motions of surge, sway and yaw of floating modules. Thus the objective function of the optimal control can be set as

$$\min J = \int_0^t \sum_i^N \left(\upsilon_{1,x} (x_i)^2 + \upsilon_{1,y} (y_i)^2 + \upsilon_{1,\gamma} (\gamma_i)^2 + \upsilon_{2,x} (\dot{x}_i)^2 + \upsilon_{2,y} (\dot{y}_i)^2 + \upsilon_{2,\gamma} (\dot{\gamma}_i)^2 \right) \mathrm{d}t$$
$$\text{s.t.} \; |\mathbf{u}_i| \leq \mathbf{u}_{i,\max} \tag{22}$$

where symbols $\upsilon_{1,x}$, $\upsilon_{1,y}$, $\upsilon_{1,\gamma}$, $\upsilon_{2,x}$, $\upsilon_{2,y}$ and $\upsilon_{2,\gamma}$ are positive coefficients to be determined. In addition, the optimal control is subjected to the constraints that the output control forces are confined within a limitation $\mathbf{u}_{i,\max}$.

Numerical methods [37,38] are used for solving the high-dimensional optimal control problem. There are two major classes, including the indirect methods and the direct methods [39]. The indirect method uses the calculus of variations to determine optimal conditions leading to a multi-point boundary-value subproblem where local extremals are identified and examined for the best solution. This calculus-based optimization method [40] might not be suitable for the high-dimensional floating system with strong nonlinearity, especially when functions of terms are discontinuous. The direct method is preferred in this paper because it deals with a complex problem simply in an iterative way. The control objective, state variables, disturbance observer and control outputs are transformed to discretized forms and the optimal control problem is turned into a nonlinear programming problem.

Considering the estimated wave disturbance, the Euler method is used to discretize the ordinary differential equations Eq. (9) and yields

$$\begin{aligned} \mathbf{x}_{1,i}^{n+1} &= \mathbf{x}_{1,i}^{n} + \delta \cdot \mathbf{x}_{2,i}^{n} \\ \mathbf{x}_{2,i}^{n+1} &= \mathbf{x}_{2,i}^{n} + \delta \cdot \left(\boldsymbol{\varphi}_i \left(\mathbf{x}_1^n, \mathbf{u}_i^n \right) + \hat{\mathbf{d}}_i^n \right) \quad i = 1, \ldots, N \\ \mathbf{x}_{1,i}^{n+2} &= \mathbf{x}_{1,i}^{n+1} + \delta \cdot \mathbf{x}_{2,i}^{n+1} \end{aligned} \tag{23}$$

where symbol δ denotes a time step and n is the iteration number of the discretized equation. The estimated disturbance in Eq. (23) also needs to be discretized based on the disturbance observer Eq. (14), given by

$$\hat{\mathbf{d}}_i^n = \left(\mathbf{w}_i^{n-1} + \delta \cdot \dot{\mathbf{w}}_i^{n-1} \right) + \mathbf{p}_i \left(\mathbf{x}_{2,i}^n \right) \quad i = 1, \ldots N \tag{24}$$

where

$$\dot{\mathbf{w}}_i^{n-1} = -\left(\left.\frac{\partial \mathbf{p}_i}{\partial \mathbf{x}_{2,i}}\right|_{\mathbf{x}_{2,i}=\mathbf{x}_{2,i}^{n-1}}\right)\left(\boldsymbol{\varphi}_i\left(\mathbf{x}_1^{n-1}, \mathbf{u}_i^{n-1}\right) + \mathbf{w}_i^{n-1} + \mathbf{p}_i\left(\mathbf{x}_{2,i}^{n-1}\right)\right) \quad i = 1, \ldots N$$

Similarly, the control objective function of Eq. (22) should be discretized as

$$\begin{aligned} \min J = \sum_i^N & \left(\upsilon_{1,x}\left(x_{1,i}^{n+2}\right)^2 + \upsilon_{1,y}\left(y_{1,i}^{n+2}\right)^2 + \upsilon_{1,\gamma}\left(\gamma_{1,i}^{n+2}\right)^2 \right. \\ & \left. + \upsilon_{2,x}\left(x_{2,i}^{n+1}\right)^2 + \upsilon_{2,y}\left(y_{2,i}^{n+1}\right)^2 + \upsilon_{2,\gamma}\left(\gamma_{2,i}^{n+1}\right)^2 \right) \\ \text{s.t. } & \left|\mathbf{u}_i^n\right| \le \mathbf{u}_{i,\max} \end{aligned} \tag{25}$$

Figure 2 shows the flowchart of the control process. In an iterative control process, the estimated wave disturbance of the nth step $\hat{\mathbf{d}}_i^n$ is based on the system state $\mathbf{x}_1^{n-1}$ and control output $\mathbf{u}_i^{n-1}$ in the $(n-1)$th step. Then the objective function Eq. (25) is optimized based on the discretized equation of the system Eq. (23), and simultaneously satisfy with the inequality constraint $\left|\mathbf{u}_i^n\right| \le \mathbf{u}_{i,\max}$. After the optimization procedure, the control output $\mathbf{u}_i^n$ of the propellers is obtained, which is applied onto the ith module at the nth step.

The dynamic optimal control problem can be solved by using the sequential quadratic programming (SQP) method [41]. This method first determines the search direction based on a subproblem of quadratic programming (QP) and then determines the search step size by using a proper merit function with the premise of convergence. The method permits the benefit of fast convergence in dealing with multivariable constrained optimization problems. In this paper, each module involves four control variables including two thrusts and two steering angles of two propellers for manipulating the modular motions, and total 4 N output control variables should be determined for each iteration step.

4 Numerical tests for verifications

In numerical experiments, we consider a floating platforms system with five semi-submersible modules that are connected by spring connectors. All the modules have the same size and all the connectors possess the same physical properties. In the first part of this section, parameters of the floating platform system and the wave parameters are given. The second part shows the control results.

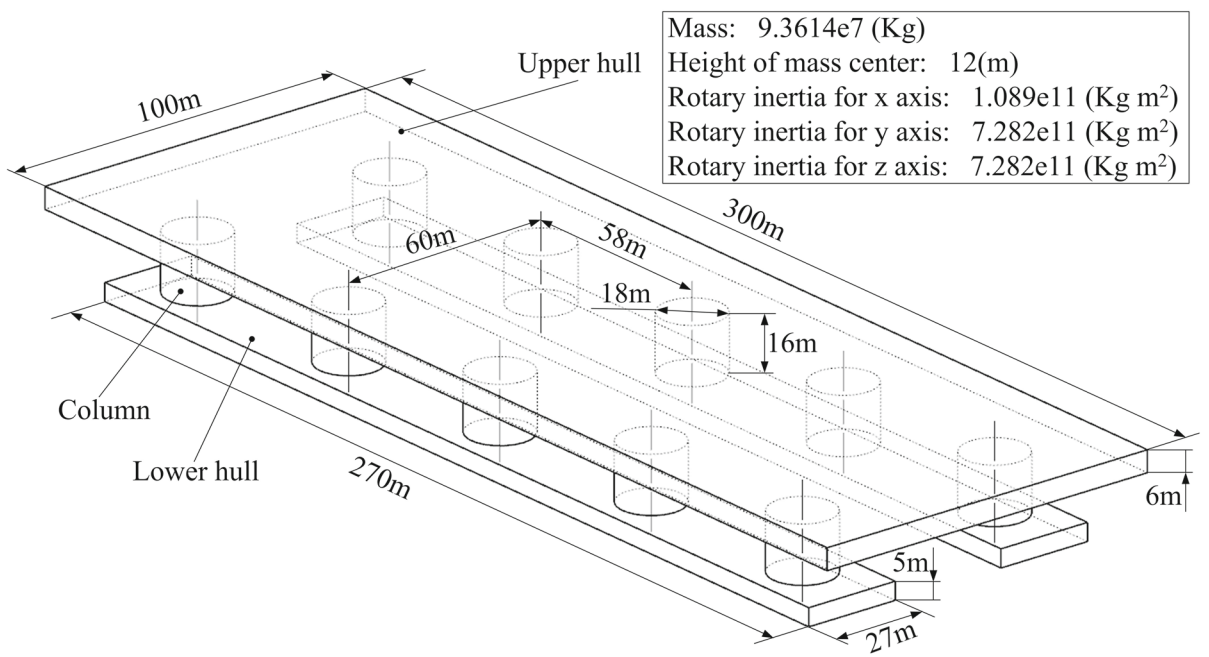

Fig. 3 Structure layout of a single floating module labeled with dimensional parameters

Table 1 Parameters of the floating system

Terms	Values
Water depth	$h = 300\,\text{m}$
Draft	$h_1 = 12\,\text{m}$
Mooring stiffness matrix	$\mathbf{D}_i = 10^7 \times \text{diag}([1, 1, 1, 100, 100, 100]^{\text{T}})\,\text{N/m}$
Initial gap between adjacent modules	$\vartheta = 25\,\text{m}$
Connector: spring stiffness	$\varepsilon = 1 \times 10^7\,\text{N/m}$
Mounting points of connector springs between two adjacent modules	Spring1 Module$i$: [150, 40, 12] Module j : [− 150, 40, 12]
	Spring2 Module i : [150,- 40, 12] Module j : [− 150, − 40, 12]
Local coordinates of installed propellers	Propeller 1 [− 100,0,− 10]
	Propeller 2 [100,0,− 10]

4.1 Preliminaries

Each module is made by one upper hull, one lower hull and ten columns. The specific parameters of a single module are shown in Fig. 3.

In numerical simulations, the floating platform consists of five floating modules which are connected by flexible connectors. The parameters of connections, location of propellers and water environment are tabulated in Table 1.

The excitation angle of wave is set to be 45°. The dominant wave frequency is $\omega_p = 1.047\,\text{rad/s}$ which corresponds to wave period of 6 s. The variation of wave height in time domain is obtained from the JONSWAP spectrum. In Eq. (8), the dimensional constant $\zeta = 0.3125$. Significant wave height H_s is set to be 3 m. The peak enhancement factor $\kappa = 3.3$. The value of peak shape parameter is dependent on the wave frequency. When $\omega \leq \omega_p, \sigma = 0.07$ and when $\omega > \omega_p, \sigma = 0.09$. Then the power spectral density of waves in Eq. (8) is shown in Fig. 4a. Accordingly, a corresponding sample of irregular wave in time domain is displayed in Fig. 4b.

The objective of the optimal control is to minimize the motions of surge, sway and yaw. Thus these three state variables are composed into the objective function in Eq. (23). However, the three state variables have different units and orders in quantity. To deal with the three terms equally impotent in the optimal process, the corresponding coefficients $\upsilon_{1,x}, \upsilon_{1,y}, \upsilon_{1,\gamma}, \upsilon_{2,x}, \upsilon_{2,y}$ and $\upsilon_{2,\gamma}$ need to be scaled in equal weight among the terms. Thus the mass and the rotational inertia of the module are used to set up the coefficients, resulting in $\upsilon_{1,x} = \upsilon_{2,x} = \upsilon_{1,y} = \upsilon_{2,y} = 9.361\text{e}7$ and $\upsilon_{1,\gamma} = \upsilon_{2,\gamma} = 7.282\text{e} + 11$. By so doing, physically, the kinetic energy dispersed into each degree of freedom is normalized in balance. To solve the optimization problem, the sequential quadratic programming is used which is a standard software package could be found in MATLAB.

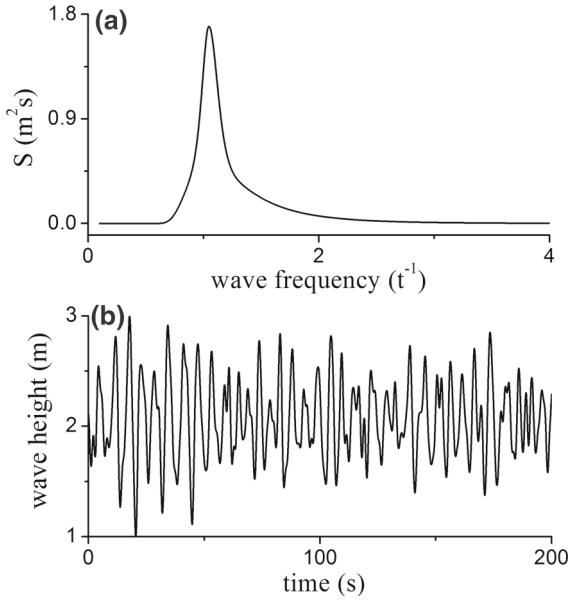

Fig. 4 **a** Power spectral density of JONSWAP wave spectrum with the parameters of $\zeta = 0.3125$, $H_s = 3\,\text{m}$, $\omega_p = 1.047\,\text{rad/s}$, $\kappa = 3.3$, $\sigma = 0.07$ for $\omega \leq \omega_p$ and $\sigma = 0.09$ for $\omega > \omega_p$. **b** A sample of irregular wave in time domain derived from the JONSWAP spectrum

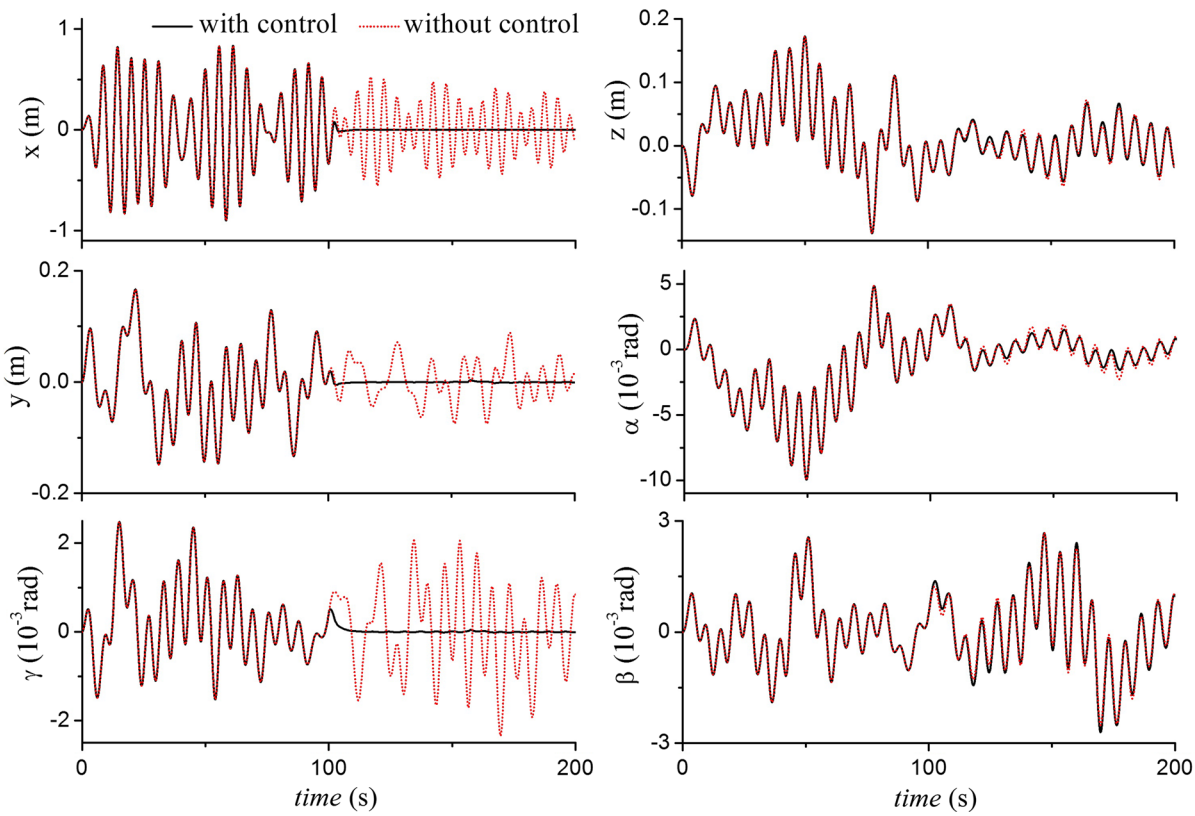

Fig. 5 Time responses of the third module with/without control

4.2 Numerical simulations

With the system parameters and the wave condition described above, the numerical simulation is carried out to test the efficiency of the control strategy. The three graphs on the left column in Fig. 5 show that the floating system initially oscillates randomly due to the excitation of uncertain waves without control. The control is switched on at 100 s, and the controlled response (solid line with black color) tends to be stabilized for the motions in x, y and γ directions, while without the control the responses (broken lines with red color) continue fluctuating in the time evolution. The control effectively reduces the amplitudes of motions of the module compared with that of the uncontrolled case. However, the control has little effect on the motions in z, β and α directions (the three graphs on the right column) because the deployment of the propellers can only actuate a vector force in the plane of X–Y. The motions of the other modules are not exhibited here since their time responses are similar to the third module.

During the control process, the loads of connectors are significantly reduced as shown in Fig. 6. It is because the connector load is associated with the relative movements of floating modules. The control suppresses the oscillations of the modules resulting in the reduction in connection loads. The loads of other springs are not shown since they are similar.

In the control process, the maximum output force is capped by 5000 KN and the turning angle of propeller covers the range of $\theta \in [-\pi, \pi]$. Figure 7 shows the thrusts of the two propellers mounted on the third module and the corresponding turning angles, respectively. Note that at the beginning of the control the absolute values of output forces of propellers are sharply truncated because of the output limitation. The actual rotational angles of the two propellers basically vary in a range of $\theta \in [+\pi/2, -\pi/2]$ to cope with the wave excitation. In this case, the maximum combined control force of two propellers is almost equivalent to the maximum wave disturbance so that the control can

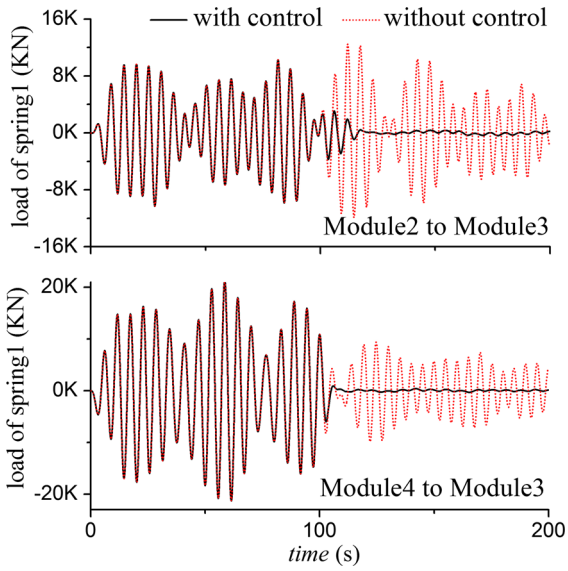

Fig. 6 Loads of the connector spring linked to the third module with/without control

effectively eliminate the motions of the module in the intended directions.

If the total combined control force is insufficient to cope with the maximum wave disturbance, the control cannot completely halt the motions of the module as shown in Fig. 8a where the motions of surge, sway and yaw are fluctuating to a certain extent during the control process. For example, if the maximum output force for each propeller is limited at 3000 KN, the controlled responses of surge, sway and yaw are not completely suppressed as shown in Fig. 8a. Meanwhile, the curves of the output control forces are frequently cut on the top or bottom extremes as indicated in Fig. 8b, implying that the control thrusts are almost fully applied on the module. The corresponding rotational angles of the propellers vary in time. Obviously in comparison with the result of Fig. 5, a larger setting of the output saturation leads to a better result of oscillation suppression.

Through the numerical experiments, we can see that the control strategy can effectively suppress the targeted motions of the floating system. In numerical tests, we have conducted many other numerical tests (not report here) to examine the performance of the control method. This control strategy generally works very well in coping with the uncertain wave conditions. It is worthwhile to note that the deployment of propellers may influence the control results. Usually if two propellers on a module are deployed farther from each other, it will result in better performance on controlling the motion of yaw since the arrangement may yield larger force arm to the rotational center of the module. We do not include the study of propeller deployment in this paper as the main task is to test the efficiency of this optimal control method applied to the multi-modular floating system. The interesting readers can refer the article [42] for the detail study of the optimal deployment of multiple propellers.

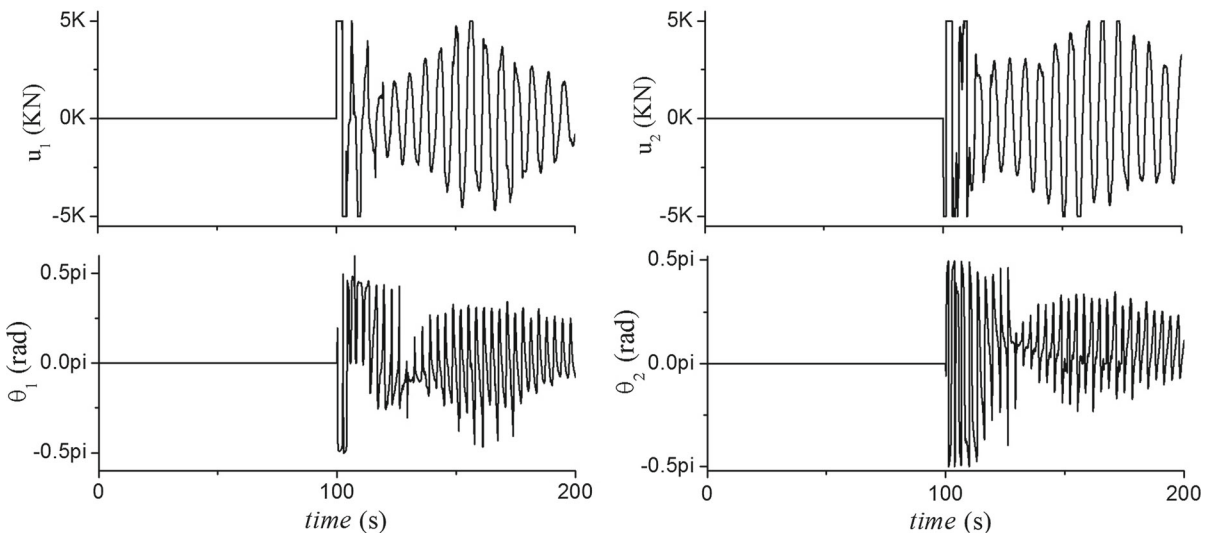

Fig. 7 Control outputs and turning angles of propellers

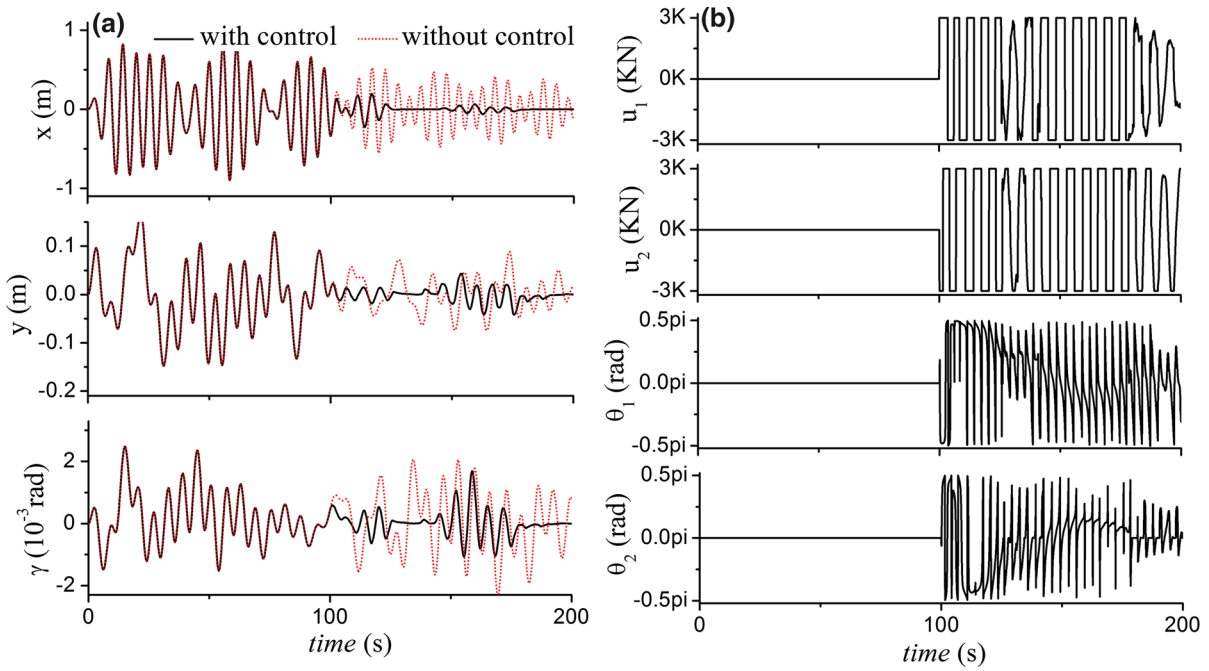

Fig. 8 A weak control process when the control output is insufficient and limited at 3000 KN. **a** Response of the third module with/without control; **b** control outputs of the thrusts and turning angles of propellers

5 Conclusions

In this paper, an adaptive optimal control method is developed to suppress the motions of a chain-type of multi-modular floating platforms in waves. A network modeling method is used to build up the control model. Irregular wave is considered which is derived from a JONSWAP spectrum. The wave excitation is assumed to be completely unknown during a control process. To cope with the uncertain waves, a wave disturbance observer associated with a feedback state of module responses is devised to estimate the actual wave excitation. This adaptive scheme of the wave estimator is integrated with an optimal control method subject to the constraint on the control outputs of propellers within a limited level. The direct optimal method is employed based on a discretized control system using the Euler method. The optimal control process is carried out in an iterative way by the sequential quadratic program method.

In numerical experiments, a multi-modular floating system is considered, which consists of five semi-submersible floating modules connected with spring connectors. On each module, the control is operated by the thrusts and turning angles of two propellers, in order to suppress the motions of surge, sway and yaw. Each module has four control variables. The control method deals with 20 control variables for controlling a 30-DOF floating system with strong geometrical nonlinearity, in addition to coping with irregular waves and control output limitation. The control is technically challenging. Numerical experiments have verified the efficiency of the control strategy. The results show that the proposed control method performs very well in an unknown random sea.

In future work, we may consider complex cases to stabilize the multi-modular system in more degrees of freedom, such as to control the z, α and β motions by rearrangement of locations of thrusts. Controlling the system in uneven sea conditions is also interested. The major contribution of this paper is the work how to handle with a high-dimensional nonlinear control problem for multi-modular floating systems. Controlling the responses of complicated systems might be very much desired in marine engineering since there is little work involving the control of vibration of multi-modular floating systems. This work might also provide an interesting example to cope with

the control of complex systems for other engineering applications.

Acknowledgements This research work was supported by the 973 Research Grant (2013CB036104), the National Natural Science Foundation of China (11472100, 11702088) and the Graduate Student Research Innovation Project of Hunan Province (CX2016B088).

Compliance with ethical standards

Conflict of interest The authors declare no conflict of interest

Human participants or animals This article does not contain any studies with human participants or animals performed by any of the authors.

Appendix

In Eq. (1), symbol $\mathbf{M}_i \in \mathbb{R}^{6\times6}$ is the mass matrix which can be defined as [43]

$$\mathbf{M}_i = \begin{bmatrix} m & 0 & 0 & 0 & 0 & 0 \\ 0 & m & 0 & 0 & 0 & 0 \\ 0 & 0 & m & 0 & 0 & 0 \\ 0 & 0 & 0 & J_x & 0 & 0 \\ 0 & 0 & 0 & 0 & J_y & 0 \\ 0 & 0 & 0 & 0 & 0 & J_z \end{bmatrix} \tag{A.1}$$

where symbol m is the mass of a single module. Symbols J_x, J_y and J_z are the rotary inertias, respectively, about x, y and z axes. Assume the coordinate of rotation center is (x_c, y_c, z_c) in local coordinate system; then, the expressions of rotary inertias are

$$\begin{aligned} J_x &= \int\int_V (y-y_c)^2 \mathrm{d}m + \int\int_V (z-z_c)^2 \mathrm{d}m \\ J_y &= \int\int_V (x-x_c)^2 \mathrm{d}m + \int\int_V (z-z_c)^2 \mathrm{d}m \\ J_z &= \int\int_V (x-x_c)^2 \mathrm{d}m + \int\int_V (y-y_c)^2 \mathrm{d}m \end{aligned} \tag{A.2}$$

The linear restoring force matrix of water $\mathbf{S}_i \in \mathbb{R}^{6\times6}$ is defined as [44]

$$\mathbf{S}_i = \begin{bmatrix} 0 & 0 & 0 & 0 & 0 & 0 \\ 0 & 0 & 0 & 0 & 0 & 0 \\ 0 & 0 & -\rho g A_w & 0 & \rho g \int\int_{A_w} x \mathrm{d}A & 0 \\ 0 & 0 & 0 & -\rho g \begin{pmatrix} V_w (z_b - z_g) \\ + \int\int_{A_w} y^2 \mathrm{d}A \end{pmatrix} & 0 & 0 \\ 0 & 0 & \rho g \int\int_{A_w} x \mathrm{d}A & 0 & -\rho g \begin{pmatrix} V_w (z_b - z_g) \\ + \int\int_{A_w} x^2 \mathrm{d}A \end{pmatrix} & 0 \\ 0 & 0 & 0 & 0 & 0 & 0 \end{bmatrix} \tag{A.3}$$

where ρ is the density of water and g is the acceleration of gravity. Symbol z_b is the height of buoyant center and z_g is the height of gravity center. Symbol A_w is the volume of the water.

In this article, a simplest linear mooring model is considered, so the mooring stiffness matrix $\mathbf{D}_i \in \mathbb{R}^{6\times6}$ is assumed as a constant matrix.

The added mass matrix $\Delta\mathbf{M}_i \in \mathbb{R}^{6\times6}$, added damping matrix $\mathbf{C}_i \in \mathbb{R}^{6\times6}$ and the magnitude vector of the excitation force of wave $\mathbf{f}_i \in \mathbb{C}^{6\times1}$ in Eq. (1) are derived through linear wave theory. By assuming that the water is irrotational and inviscid, the total wave potential can be written as

$$\chi = \chi_I + \chi_D + \delta\omega \sum_{i=1}^{N} (\chi_i)^{\mathrm{T}} \bar{\mathbf{x}}_{1,i} \tag{A.4}$$

where $\delta = \sqrt{-1}$, symbols χ_I and χ_D are the incident potential and diffraction potential. Vector $\boldsymbol{\chi}_i = \left[\chi_i^1, \chi_i^2, \ldots, \chi_i^6\right]^{\mathrm{T}}$ is the potential of the ith module produced by the unit amplitude of each degree of freedom. Vector $\bar{\mathbf{x}}_{1,i}$ is the complex amplitude of the ith module. The incident potential χ_I can be expressed as

$$\chi_I = \frac{\delta g a}{\omega} \frac{\cosh k\,(z+h)}{\cosh\,(kh)} e^{\delta k(x\cos\theta + y\sin\theta)} \tag{A.5}$$

where ω, a, θ and h are wave frequency, wave height, exciting angle and water depth, respectively. Symbol k is the wave number which is related to ω and h. Diffraction potential χ_D and potential vector $\boldsymbol{\chi}_i$ satisfy Laplace equation and the conditions of free surface, body's surface boundary, sea bottom and infinity radiation and can be solved by the boundary element method. (In this paper, HydroD is applied.) After, through Bernoulli's equation, the amplitude of wave force is obtained by integrating the wave potential along the wet surface

$$\begin{aligned}\bar{\mathbf{f}}_{w,i} &= \int\int_{S_i}\left[-\delta\omega\rho\left(\chi_I+\chi_D+\delta\omega\sum_{j=1}^{N}(\boldsymbol{\chi}_j)^{\mathrm{T}}\bar{\mathbf{x}}_{1,j}\right)\right]\mathbf{n}_i ds\\ &= -\delta\omega\rho\int\int_{S_i}(\chi_I+\chi_D)\mathbf{n}_i ds\\ &\quad+\rho\omega^2\sum_{j=1}^{N}\left(\int\int_{S_i}\left[\mathrm{Re}\left((\boldsymbol{\chi}_j)^{\mathrm{T}}\right)\bar{\mathbf{x}}_{1,j}\mathbf{n}_i\right.\right.\\ &\quad+\left.\left.\delta\mathrm{Im}\left((\boldsymbol{\chi}_j)^{\mathrm{T}}\right)\bar{\mathbf{x}}_{1,j}\mathbf{n}_i\right]\mathrm{d}s\right)\end{aligned}\tag{A.6}$$

$$\boldsymbol{\Phi}=\begin{bmatrix}0&1&0&\cdots&0\\1&0&1&\ddots&\vdots\\0&1&0&\ddots&0\\\vdots&\ddots&\ddots&\ddots&1\\0&\cdots&0&1&0\end{bmatrix}\tag{A.10}$$

The relative displacement vector $K\left(\mathbf{x}_{1,i},\mathbf{x}_{1,j}\right)\mathbb{R}^{6\times1}$ is

$$K\left(\mathbf{x}_{1,i},\mathbf{x}_{1,j}\right)=\sum_{m=1}^{N_c}\left[\begin{array}{c}\left(\left\|\mathbf{p}_{2j,m}-\mathbf{p}_{1i,m}\right\|-\vartheta\right)\frac{\mathbf{p}_{2j,m}-\mathbf{p}_{1i,m}}{\left\|\mathbf{p}_{2j,m}-\mathbf{p}_{1i,m}\right\|}\\ \left\{\left(\left\|\mathbf{p}_{2j,m}-\mathbf{p}_{1i,m}\right\|-\vartheta\right)\frac{\mathbf{p}_{2j,m}-\mathbf{p}_{1i,m}}{\left\|\mathbf{p}_{2j,m}-\mathbf{p}_{1i,m}\right\|}\right\}\times\left(\mathbf{p}_{1i,m}-\mathbf{p}_{a,i}\right)\end{array}\right]\tag{A.11}$$

where $\mathbf{n}_i=\left[n_i^1,n_i^2,\ldots,n_i^6\right]^{\mathrm{T}}$ whose elements indicates pth projection component of the outward normal vector and S_i is the wet surface.

The wave force is assumed as harmonic excitation and the response of floating system is harmonic too. Then we have

$$\begin{aligned}\mathbf{f}_{w,i}&=\bar{\mathbf{f}}_{w,i}e^{-i\omega t}\\ \mathbf{x}_{1,j}&=\bar{\mathbf{x}}_{1,j}e^{-i\omega t}\\ \dot{\mathbf{x}}_{1,j}&=-\delta\omega\bar{\mathbf{x}}_{1,j}e^{-i\omega t}\\ \ddot{\mathbf{x}}_{1,j}&=-\omega^2\bar{\mathbf{x}}_{1,j}e^{-i\omega t}\end{aligned}\tag{A.7}$$

Rewriting Eq. (A.6) to a matrix form and substituting Eq. (A.7) into Eq. (A.6), we have

$$\mathbf{f}_{w,i}=\mathbf{f}_i e^{-i\omega t}-\sum_{j=1}^{N}\left(\Delta\mathbf{M}_j\ddot{\mathbf{x}}_{1,j}+\Delta\mathbf{C}_j\dot{\mathbf{x}}_{1,j}\right)\tag{A.8}$$

where

$$\begin{aligned}\mathbf{f}_i&=-\delta\omega\rho\int\int_{S_i}\left(\chi_I+\chi_D\right)\mathbf{n}_i\mathrm{d}s\\ \Delta\mathbf{M}_j&=\rho\int\int_{S_i}\mathrm{Re}\left(\boldsymbol{\chi}_j\right)\mathbf{n}_i^T\mathrm{d}s\\ \Delta\mathbf{C}_j&=\rho\omega\int\int_{S_i}\mathrm{Im}\left(\boldsymbol{\chi}_j\right)\mathbf{n}_i^T\mathrm{d}s\end{aligned}\tag{A.9}$$

In Eq. (1), the term $\varepsilon\sum_{j=1}^{N}\left(\boldsymbol{\Phi}_{ij}K\left(\mathbf{x}_{1,i},\mathbf{x}_{1,j}\right)\right)$ denotes the connector forces imposed on the ith module. For chain-type modular floating platforms, the topological matrix $\boldsymbol{\Phi}\in\mathbb{R}^{N\times N}$ is defined by

where N_c is the number of springs in a connector between two adjacent modules. Symbols $\mathbf{p}_{1i,m}$ and $\mathbf{p}_{2j,m}$ are the moving positions of the mounting points of the mth spring, respectively, on the ith module and jth module under wave excitation. Symbol $\mathbf{p}_{a,i}$ is the mass center coordinate of the ith module when the system moves. Symbol ϑ indicates the initial gap between two adjacent modules. The displacement vector of the ith module is $\mathbf{x}_{1,i}=[x_i,y_i,z_i,\alpha_i,\beta_i,\gamma_i]^{\mathrm{T}}$. Then symbols $\mathbf{p}_{1i,m}$, $\mathbf{p}_{2j,m}$ and $\mathbf{p}_{a,i}$ can be written as

$$\begin{aligned}\mathbf{p}_{a,i}&=\mathbf{p}_{0,i}+[x_i,y_i,z_i]^{\mathrm{T}}\\ \mathbf{p}_{1i,m}&=\mathbf{p}_{a,i}+\mathrm{tran}\left(\alpha_i,\beta_i,\gamma_i\right)\cdot\mathbf{p}_{1i,m}^0\\ \mathbf{p}_{2j,m}&=\mathbf{p}_{a,j}+\mathrm{tran}\left(\alpha_j,\beta_j,\gamma_j\right)\cdot\mathbf{p}_{2j,m}^0\end{aligned}\tag{A.12}$$

where $\mathbf{p}_{1i,m}^0$ and $\mathbf{p}_{2j,m}^0$ are, respectively, the coordinates in body-fixed reference of two mounting points of the ith and the jth modules. Symbol $\mathbf{p}_{0,i}$ is the initial position of the mass center of the ith module when the floating platform is in still water. Function tran $(\cdot)$ is a coordinate transfer function [30].

References

1. Wang, C.M., Watanabe, E., Utsunomiya, T.: Very Large Floating Structures. CRC Press, Boca Raton (2007)
2. Wang, C.M., Tay, Z.Y.: Very large floating structures: applications, research and development. Procedia Eng. **14**, 62–72 (2011)
3. Lamas-Pardo, M., Iglesias, G., Carral, L.: A review of very large floating structures (VLFS) for coastal and offshore uses. Ocean Eng. **109**, 677–690 (2015)
4. Kashiwagi, M.: Research on hydroelastic responses of VLFS: recent progress and future work. Int. J. Offshore Polar Eng. **10**, 81–90 (2000)
5. Ohmatsu, S.: Overview: research on wave loading and responses of VLFS. Mar. Struct. **18**, 149–168 (2005)

6. Bishop, R.E.D., Price, W.G.: Hydroelasticity of Ships. Cambridge University Press, Cambridge (1979)
7. Kashiwagi, M.: A B-spline Galerkin scheme for calculating the hydroelastic response of a very large floating structure in waves. J. Mar. Sci. Technol. **3**, 37–49 (1998)
8. Riggs, H.R., Ertekin, R.C.: Approximate methods for dynamic response of multi-module floating structures. Mar. Struct. **6**, 117–141 (1993)
9. Liu, X., Sakai, S.: Time domain analysis on the dynamic response of a flexible floating structure to waves. J. Eng. Mech. **128**, 48–56 (2002)
10. Falnes, J.: Optimum control of oscillation of wave-energy converters. Int. J. Offshore Polar Eng. **12**, 147–155 (2002)
11. Nie, R., Scruggs, J.T.: Disturbance-adaptive stochastic optimal control of energy harvesters, with application to ocean wave energy conversion. IFAC Proc. **47**, 7702–7709 (2014)
12. Healey, A.J., Lienard, D.: Multivariable sliding mode control for autonomous diving and steering of unmanned underwater vehicles. IEEE J. Ocean. Eng. **18**, 327–339 (1993)
13. Alarçïn, F.: Internal model control using neural network for ship roll stabilization. J. Mar. Sci. Technol. **15**, 141–147 (2007)
14. Li, H.J., Hu, S.-L.J., Jakubiak, C.: H 2 active vibration control for offshore platform subjected to wave loading. J. Sound Vib. **263**, 709–724 (2003)
15. Luo, M., Zhu, W.Q.: Nonlinear stochastic optimal control of offshore platforms under wave loading. J. Sound Vib. **296**, 734–745 (2006)
16. Christiansen, S., Knudsen, T., Bak, T.: Extended onshore control of a floating wind turbine with wave disturbance reduction. J. Phys. Conf. Ser. **555**, 012018 (2014)
17. Zhang, B.-L., Han, Q.-L., Zhang, X.-M., Yu, X.: Integral sliding mode control for offshore steel jacket platforms. J. Sound Vib. **331**, 3271–3285 (2012)
18. Xia, Y., Xu, G., Xu, K., Chen, Y., Xiang, X., Ji, Z.: Dynamics and control of underwater tension leg platform for diving and leveling. Ocean Eng. **109**, 454–478 (2015)
19. Faÿ, H.: Dynamic Positioning Systems: Principles, Design and Applications. Editions Technip, Paris (1990)
20. Sørensen, A.J.: A survey of dynamic positioning control systems. Annu. Rev. Control. **35**, 123–136 (2011)
21. Fossen, T.I.: Guidance and Control of Ocean Vehicles. Wiley, New York (1994)
22. Stephens, R.I., Burnham, K.J., Reeve, P.J.: A practical approach to the design of fuzzy controllers with application to dynamic ship positioning. IFAC Proc. **28**, 370–377 (1995)
23. Fossen, T.I., Grovlen, A.: Nonlinear output feedback control of dynamically positioned ships using vectorial observer backstepping. IEEE Trans. Control Syst. Technol. **6**, 121–128 (1998)
24. Manikonda, V., Gopinathan, M., Arambel, P., Mehra, R.K.: Nonlinear model predictive control design for coordinated dynamic positioning of a multi-platform mobile offshore base. In: Proceedings of the Third International Workshop on Very Large Floating Structures (1999)
25. Amin, J., Mehra, R.K., Arambel, P.: Coordinated dynamic positioning of a multi-platform mobile offshore base using nonlinear model predictive control. In: The Eleventh International Offshore and Polar Engineering Conference. International Society of Offshore and Polar Engineers (2001)
26. Hirayama, T., Ma, N.: Dynamic response of a very large floating structure with active pneumatic control. In: Proceedings of the Seventh International Offshore and Polar Engineering Conference (1997)
27. Xia, S.Y., Xu, D.L., Zhang, H.C., Qi, E.R., Hu, J.J., Wu, Y.S.: On retaining a multi-module floating structure in an amplitude death state. Ocean Eng. **121**, 134–142 (2016)
28. Bar-Eli, K.: Coupling of chemical oscillators. J. Phys. Chem. **88**, 3616–3622 (1984)
29. Zhang, H.C., Xu, D.L., Xia, S.Y., Lu, C., Qi, E.R., Tian, C., Wu, Y.S.: Nonlinear network modeling of multi-module floating structures with arbitrary flexible connections. J. Fluids Struct. **59**, 270–284 (2015)
30. Loukogeorgaki, E., Angelides, D.C.: Stiffness of mooring lines and performance of floating breakwater in three dimensions. Appl. Ocean Res. **27**, 187–208 (2005)
31. Zhang, H., Xu, D., Lu, C., Qi, E., Hu, J., Wu, Y.: Amplitude death of a multi-module floating airport. Nonlinear Dyn. **79**, 2385–2394 (2015)
32. Xu, D.L., Zhang, H.C., Lu, C., Qi, E.R., Tian, C., Wu, Y.S.: Analytical criterion for amplitude death in nonautonomous systems with piecewise nonlinear coupling. Phys. Rev. E. **89**, 042906 (2014)
33. Onorato, M., Osborne, A.R., Serio, M., Bertone, S.: Freak waves in random oceanic sea states. Phys. Rev. Lett. **86**, 5831 (2001)
34. Newland, D.E.: Random Vibrations and Spectral Analysis. Springer, Berlin (1975)
35. Deshpande, V.S., Phadke, S.B.: Control of uncertain nonlinear systems using an uncertainty and disturbance estimator. J. Dyn. Syst. Meas. Control. **134**, 24501 (2012)
36. Chen, W.-H.: Nonlinear disturbance observer-enhanced dynamic inversion control of missiles. J. Guid. Control. Dyn. **26**, 161–166 (2003)
37. Bryson, A.E.: Applied Optimal Control: Optimization, Estimation and Control. CRC Press, Boca Raton (1975)
38. Rao, A.V.: A survey of numerical methods for optimal control. Adv. Astronaut. Sci. **135**, 497–528 (2009)
39. Schwartz, A.L.: Theory and implementation of numerical methods based on Runge–Kutta integration for solving optimal control problems. University of Califomia (1996)
40. Bellman, R.: Dynamic programming and Lagrange multipliers. Proc. Natl. Acad. Sci. **42**, 767–769 (1956)
41. Nocedal, J., Wright, S.J.: Sequential Quadratic Programming. Springer, Berlin (2006)
42. Webster, W.C., Sousa, J.: Optimum allocation for multiple thrusters. In: The Ninth International Offshore and Polar Engineering Conference. International Society of Offshore and Polar Engineers (1999)
43. Faltinsen, O.: Sea Loads on Ships and Offshore Structures. Cambridge University Press, Cambridge (1993)
44. El-Hawary, F.: The Ocean Engineering Handbook. CRC Press, Boca Raton (2000)